Original article

Head, chest and femur injury in teenage pedestrian–SUV crash; mass influence on the speeds

Filippo Carollo[1], Gabriele Virzì Mariotti[2], Vincenzo Naso[1] and Salvatore Golfo[2]

Abstract

This work studies the teenage pedestrian–sport utility vehicle (SUV) crash; injury to the vital parts of the body, such as the head and chest, and to the femur is evaluated. More advanced injury criteria are applied, as provided in the rules. The multibody technique is applied by making use of SimWise software and of the teenager anthropomorphic model, the use of which is now consolidated. Head injury criterion (HIC) is used for the head, thoracic trauma index (TTI) criterion for the thorax in the case of side impact and 3 ms criterion in the case of frontal impact, while the force criterion is used for the femur. Both the TTI and femur load evaluation require non-substantial modifications of the dummy, by insertion of sensors for the measurement of the acceleration of the 4th rib and the 12th vertebra and two very thin plates at the knees for the correct individuation of the contact point with the vehicle bumper. Particular attention is paid to the front shape of the vehicle, concluding that the SUV examined in this paper is less dangerous than the sedan studied in a previous work, since its frontal dimensions (bonnet angle, bumper height and bonnet height) are more advantageous. However the teenage pedestrian in a lateral position is less prone to injuries in the head and chest, with respect to the frontal position; the pedestrian's position has little influence on femur damage. Furthermore, the braking of the vehicle reduces the possibility of crash fatality. In conclusion, a theoretical approach is shown, to highlight the influence of the vehicle mass on the pedestrian speed after the impact.

Introduction

Many works can be found in the literature on the impact of a vehicle on a teenager[1,2] or adult pedestrian;[3–14] furthermore, numerous works study the impact of the vehicle on the adult cyclist[15–21] or both cyclist and pedestrian.[17,22–27] In addition, more recently papers can be found in the literature on accidents between vehicles and the teenage cyclist.[28–34] The necessity of studies in this field has been highlighted by Neilson,[35] who concluded that the opportunity exists to introduce measures for the protection of pedestrians and the legs of motorcyclists, and to include the latest advances in the protection of car occupants. In Mukerjee et al. the authors indicate that car-mounted countermeasures, designed to mitigate pedestrian injury, have the potential to be effective even for cyclists.[21] In general, the rules indicate the

characteristics of the dummies for crash evaluation,[36–39] or the impactor characteristics for the head and leg injury evaluation.[40–42] The teenager anthropomorphic model is defined a previous paper[1] as a derivation of the adult dummy representing the 50th percentile. The applied simulation method is a multibody technique; the most widely used programs are MADYMO, Aprosys and PC Crash, while Simpack is used in[12] and SimWise is effectively used in this paper, using the indirect approach.

[1]DIMA, University of Roma La Sapienza, Italy
[2]DIID, Palermo University, Italy

Corresponding author:
Gabriele Virzì Mariotti, DIID, Palermo University, Viale delle Scienze, ed. 8, Palermo, Italy.
Email: gabriele.virzimariotti@unipa.it

The topic of vehicle front influence is frequently found in the literature, but only in recent times. Previous work[43] examines the influence of the vehicle's frontal part in general, while other works also address the crash involving the sport utility vehicle (SUV) and a cyclist or pedestrian[8,21,26]; but only in the paper by Carollo[44] is the teenage cyclist–pick-up impact found. This extends the results already achieved in the other papers[28,29,33] where the injuries caused by the energy impact of a sedan on a teenage cyclist are taken into account and analysed. In Carollo et al. an analogous crash is studied in the case of a SUV,[31,32] instead of a normal sedan: references are found only to an adult or a child, in many cases without taking into account the type of vehicle. Schebalová et al. studied the impact of a passenger vehicle on a P6 dummy. [45] In Lee et al.,[46,47] the authors investigated the deployment time (or response time) of an active hood lift system (AHLS) of a passenger vehicle activated by a gunpowder actuator, while four vehicle types, including large and compact passenger cars, minivans and light trucks, are simulated in Liu et al.[48] according to their frequency of involvement in real world accidents. The influences of various front shapes of vehicles and compliance parameters are analysed, along with possible counter measures on the basis of vehicle front design, to mitigate the severity of injury to the pedestrians, are discussed. Han et al. studies the collision of four different vehicle types with the pedestrian, concluding that the vehicle impact velocity and vehicle front-end shape are the two dominant factors influencing the pedestrian kinematics and injury severity. [49] Vehicle designs consisting of a short front-end and a wide windshield area can protect pedestrians from fatalities. Li et al. shows the influence of numerous parameters of the front shape of the vehicle. [50] Also in Sankarasubramanian et al.,[51] the authors conclude that bonnet leading edge has to be located at a height of 0.74 m from ground and propose other measures; and in effect, the paper prepared by Carollo et al.[52] lays emphasis on impact with the cyclist only. Shen et al. reports the reconstruction of real accidents and techniques for the analysis of the results. [53] The Monte Carlo technique is applied in Wood et al. to determine the impact speed, and the results are compared with actual cases. [9]

Chest speed data of the previous simulations are analysed in Carollo et al., in order to quantify the influence of the front part of the vehicle on injury to the cyclist. [52] The result is obtained using all the crash data and a theoretical approach is adopted for the study of the vehicle crash in the case of a fully elastic collision, with very good results. The theoretical approach allows the understanding of the influence of the vehicle mass on the chest contact speed; a criterion is given to determine the best value of some parameters of the vehicle front part. No other paper on the influence of the mass of the vehicle is found in literature, with the exception of Carollo et al.,[34,35]. Particular attention is devoted to the bumper in the frontal shape, because it influences the injury to not only the femur and legs, but also to the chest and head. Detweiler and Miller show the development of a front bumper system in their paper. [7]

A paper by Chakravarthy et al. indicates that pedestrian collisions remain the second leading cause of unintentional, injury-related deaths among children in the 5–14 age group. [55] Children under 15 account for 8% of all pedestrian deaths in the United States.

This work extends the results obtained in previous papers.[1,3] Bellavia and Virzi Mariotti.[3] show the vehicle–pedestrian crash, while Virzi Mariotti and Golfo[1] show the results of the teenage pedestrian–vehicle crash, evaluating the damage to the head and the thorax; in this paper a direct comparison is made using a SUV vehicle instead of a sedan, analysing not only the head and thorax injuries, but also the femur injury, using the force injury criteria. Moreover the theoretical approach shown for the cyclist speed impact in the previous paper is also validated for the pedestrian.

Implementation of the teenage pedestrian anthropomorphic model and SUV virtual model

The teenage pedestrian anthropomorphic model has been used in previous simulations, as in the case of the adult pedestrian and the teenage cyclist. The simulation technique is the same, through adequate testing in SimWise room. The vehicle is a SUV, but the model and manufacturer are different from those in the previous papers;[31,32] the information on the characteristic data are given by the manufacturer and the vehicle mass is 2270 kg.

Sketchup software was used to obtain the CAD model; it was imported in SimWise, attributing the correct value to all the essential parameters. Figure 1 shows the vehicle, and Figure 2 shows the particulars of the vehicle front shape. In this phase of the study, only three fundamental parameters were chosen for the impact fatality, compared to other works in the literature; this choice limits the number of possible combinations.

Biomechanics of the impacts and femur injury criteria

Biomechanics[56–58] is the discipline of applying the principles of mechanics to living organisms; it deals with the description of the movement of several body parts and the evaluation of the forces acting on them. Biomechanics is involved in the forecast and prevention of injury to the human body, facilitating the development of vehicle safety; it is needed to study models to evaluate the gravity of the injury. This branch of biomechanics is the starting point of passive safety. Previous research has shown that in many cases, the injury gravity is attributable to the accelerations produced by the crash.
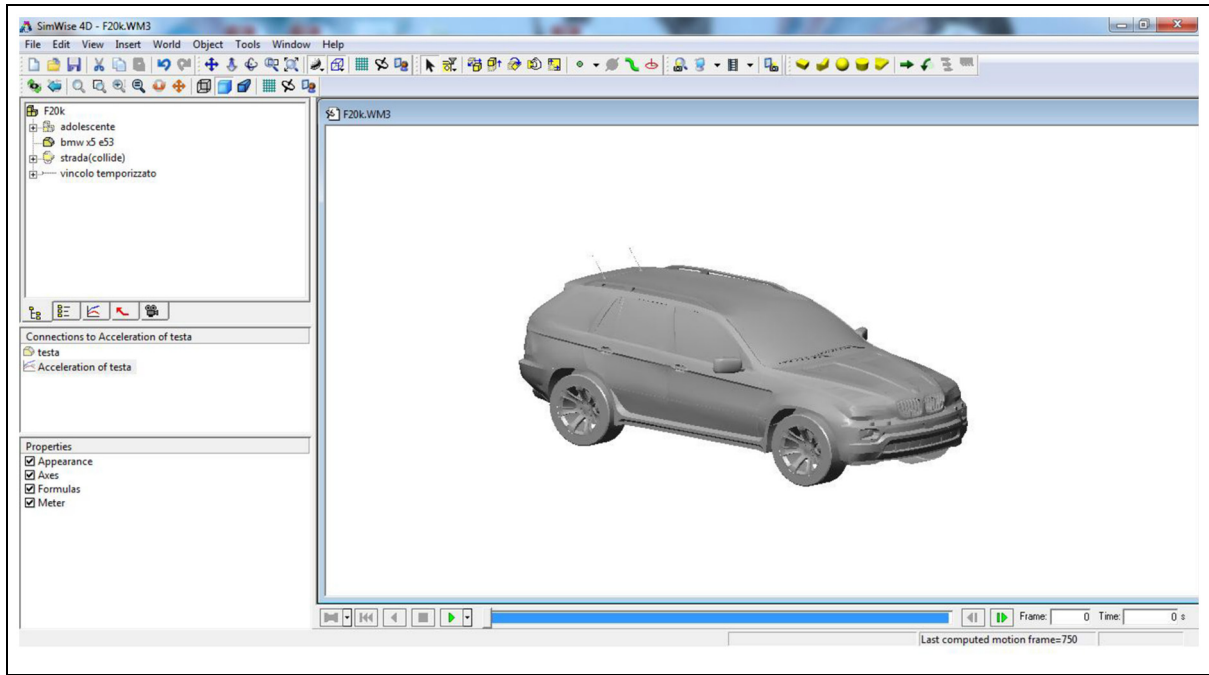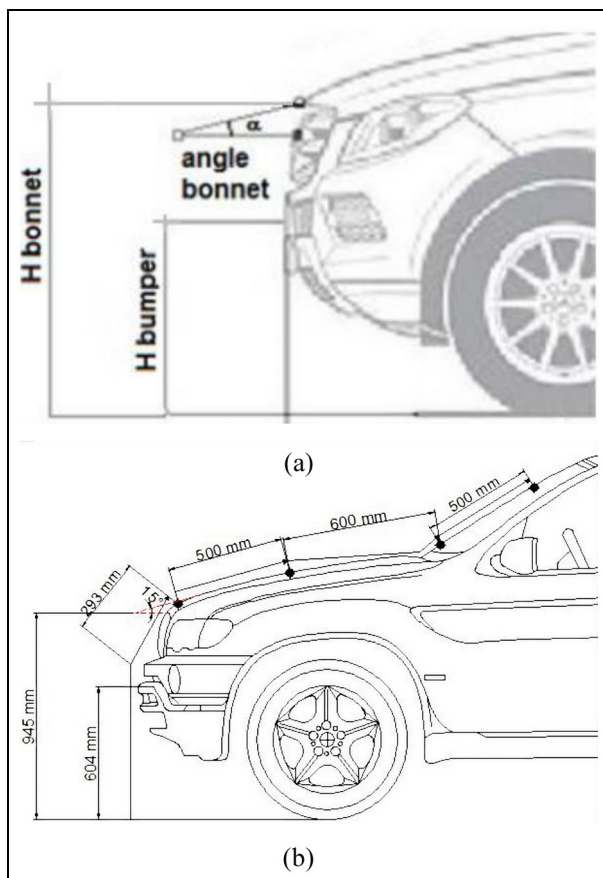
Figure 1. SUV in SimWise environment.

Figure 2. (a) Geometric parameters and (b) particulars of the front shape.

The abbreviated injury scale (AIS) and the parameters used in respect of injury to the head and the thorax are described in previous works.[1]

Leg injuries constitute the most frequent trauma in crashes involving the pedestrian, cyclist and motorcyclist. The femur is involved in 19% of road crashes and the displacement of the fragments depends on the collision intensity and on the media crushed against the femur. Usually the trauma is revealed in the kinetic energy effect, emphasized by the instinctive muscular contraction. Acceptance levels are inserted in the final relation of the European Experimental Vehicles Committee (EEVC) WG10,[36] on the basis of biomechanical study and accident reconstructions, proposing the following limits for all the test methods regarding the inferior legs:

- Foot/knee
  - Knee: maximum lateral bend angle 15°;
  - Knee: maximum displacement 6 mm;
  - Tibia: maximum lateral acceleration 150 g.
- Thigh
  - Maximum immediate sum of the femur forces 4 kN; and
  - Maximum bending moment in the femur 220 Nm.

The criterion used in this paper is the immediate sum of the forces on the femur, since it is the most compatible with the adopted simulation software. In this case, the different kinds of femur injury are distributed in the AIS scale shown in Table 1.

Table 1. AIS values of femur injury.

AIS	Description
1	Contusion to the soft tissue
2	Knee dislocation, tendon laceration, bone fractures, pelvis fracture
3	Femur fracture, pelvis fracture and aperture, knee break
4	Knee amputation, pelvis complete aperture
5	Crushing of bones, vascular break

Simulation of teenage pedestrian–vehicle crash

Generally, the pedestrian is considered to be in a perpendicular direction to the longitudinal axis of the road, with an orthogonal and negligible speed, in relation to the vehicle coming up. Simulations are executed considering the teenager in two different positions.

1. The pedestrian is motionless on the roadway, with his side towards the vehicle coming up.
2. The pedestrian is found against the vehicle, on his feet and motionless.

The action of the car brakes, which involves a decrease in vehicle speed, may not be really beneficial for the bump evolvement. In fact, though by decreasing the speed, the impact on pedestrians is certainly smaller, it must also be considered that given the time of perception and reaction of the driver, the slowing is often very poor. Assuming the time of physical-mechanical delays to have already elapsed and considering a good braking ability of the vehicle to impose a deceleration of 0.6 g (at the limit of breakage of the adherence conditions in the case of asphalt), most of the time the braking action occurs when the impact has already taken place or is happening.

The objective of this research is the calculation of head injury criterion (HIC) for the head injury, thoracic trauma index (TTI) for the chest injury with the teenager in lateral position, 3 ms criterion for the evaluation of the thorax injury with the teenager in frontal position and the contact force on the femur, when the teenager is found in lateral or frontal position in relation to the vehicle. The principal conditions constituting the dynamics of the teenage pedestrian–vehicle impact are reconstructed following the protocol EEVC-17.

The simulations are executed in a standard way at speeds 20, 30, 40 and 50 km/h, while simulation results at 10 km/h are used for the femur only. Parameters measured during the simulations are as follows.

1. Acceleration in the head centre.
2. Acceleration in the thorax gravity centre.
3. Acceleration of 4th rib and 12th vertebra.
4. Contact force on the femur.
5. Maximum speed of the head and the thorax.
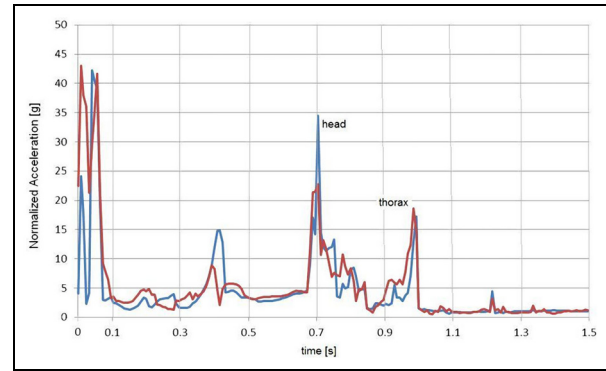
**Figure 3.** Lateral impact at V = 30 km/h in braking.

An example of the acceleration trend of the thorax and head versus the time is shown in Figure 3. Figure 4 shows the trajectory of the pedestrian in the crash at 20 km/h; he is placed in front of a vehicle that is deploying the brakes; the forward projection of the pedestrian can be noted. Figure 5 shows a similar case with the vehicle at a constant speed of 20 km/h; one can note the phase of loading on the bonnet and a gradual release on the ground. Figure 6 shows the simulation at the constant speed of 50 km/h, in the side impact; one can note the phase of loading on the bonnet and the subsequent vault, that is typical of high speed accidents. Figure 7 is similar, with the difference that the vehicle is in the process of braking.

Results analysis

HIC calculation

Simulations furnish a large volume of data. Table 2 shows the synthesis of results and HIC values are calculated with a base of 36 ms, as per the rules. The fatality percentage of the event is determined by correlating the HIC results with the injury scale AIS. Figure 8 shows the HIC–AIS correlation of the four conditions of impact; the fatality percentage is also reported in Table 2.

From the qualitative point of view, the time-acceleration diagrams (Figure 3) are very similar to those obtained with the sedan, even if the acceleration values and the times are different. HIC values can be compared with those obtained by other researchers. In particular, 188 pedestrian accidents, selected from several databases, were studied by Yang et al.[12] and the accidents were reconstructed by MADYMO. The researchers distinguished between adults and children, without taking into account other factors such as the compliance and the shape of the bonnet, the relative positions and the pedestrian speed and braking, by relating the HIC value to the impact velocity. These results were statistically interpolated by curves of the second order. The equation for children is
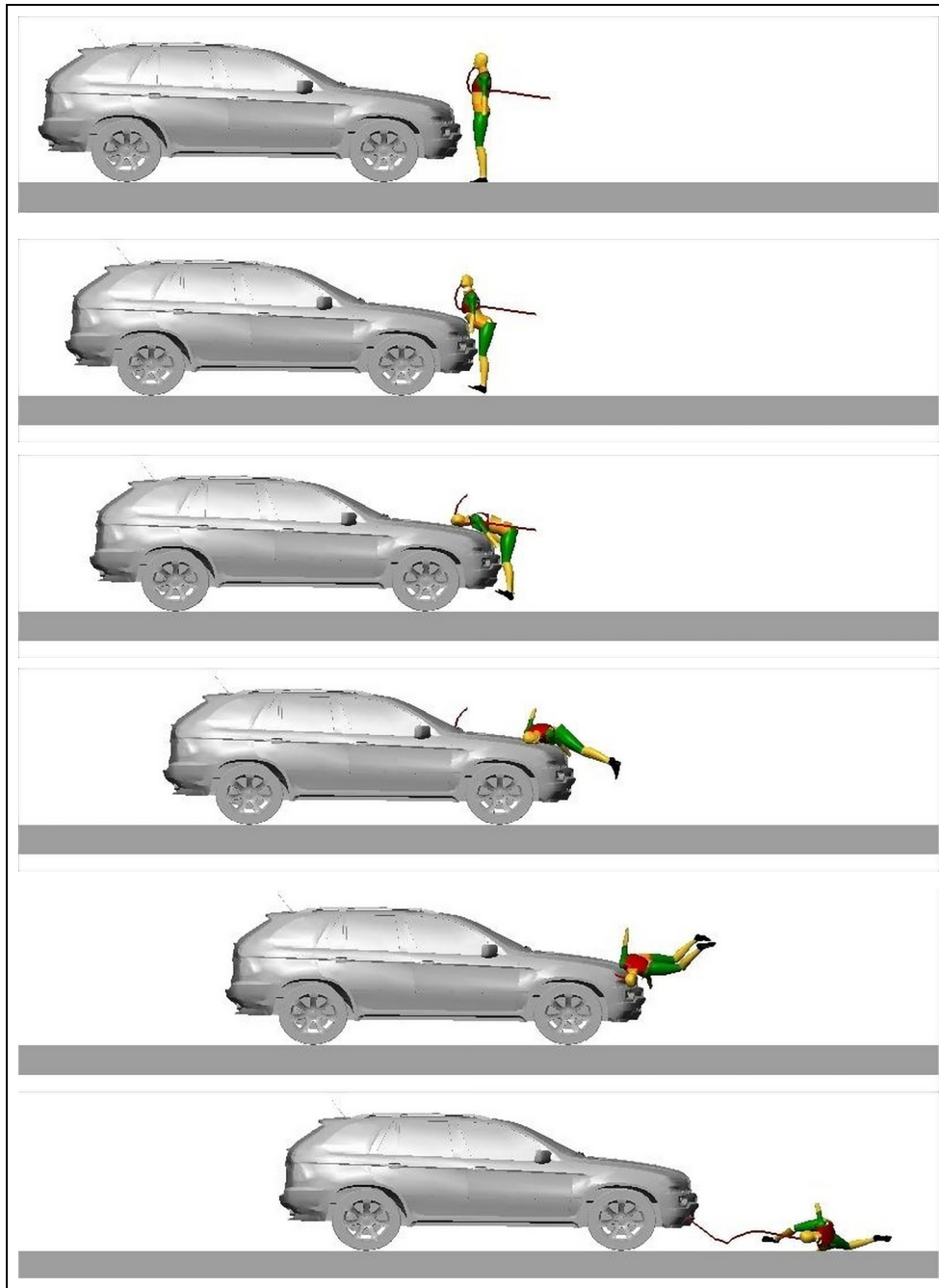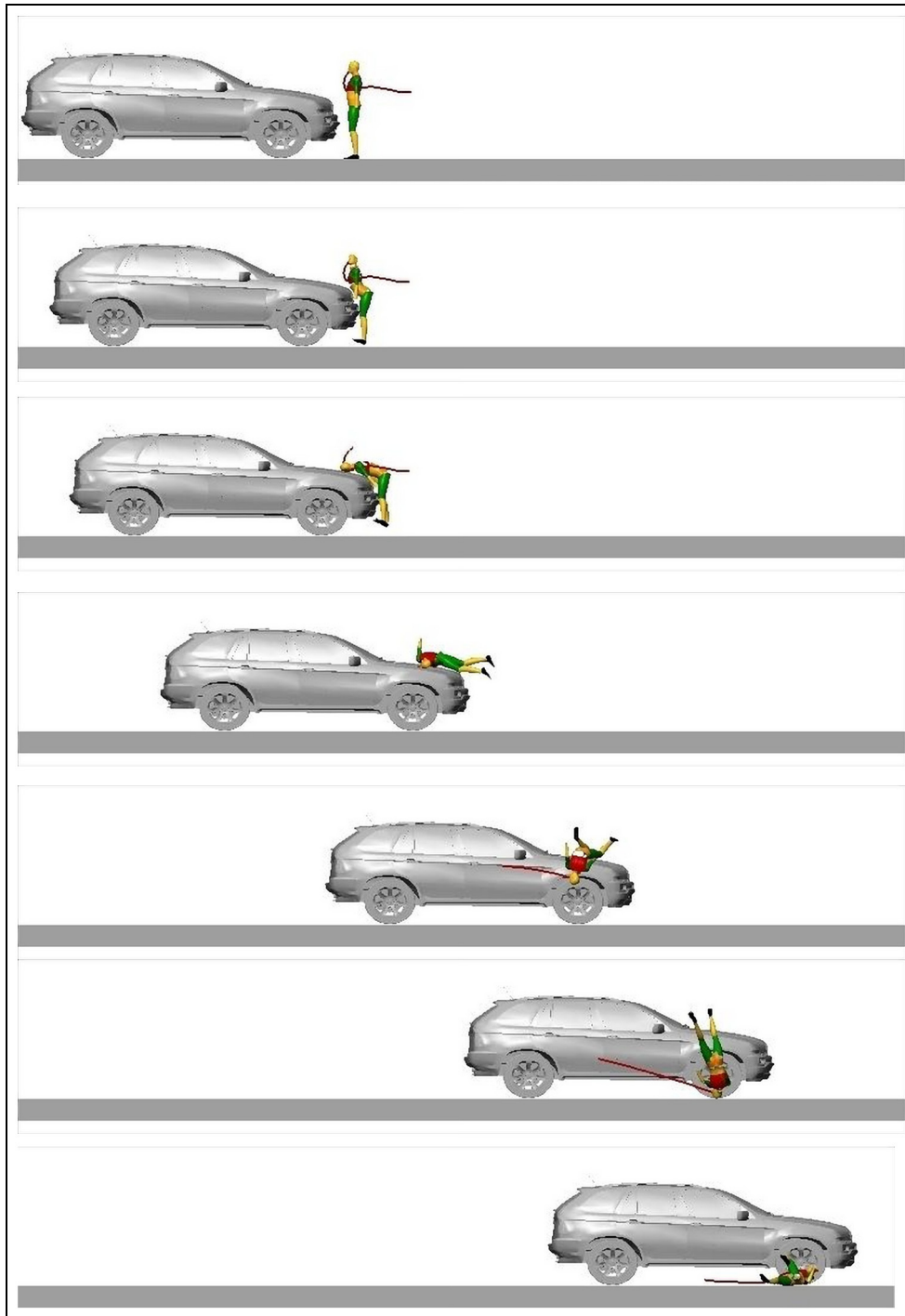
Figure 4. Frontal Impact at 20 km/h with braking. The sequence from the beginning of the impact until the end is shown in six time intervals.

$$HIC = 0.2169V^2 + 46.141V - 1046.2, R^2 = 0.974 \quad (1)$$

The independent variable V is the impact speed [km/h] and R^2 is the variance. A 'child' is an individual younger than a teenager (i.e. less than 13).

The following HIC values are reported in Figure 9(a): the relationship (1), the mean data obtained for the sedan in Virzi Mariotti and Golfo,[1] the mean data obtained for the SUV in this work, the data obtained for the SUV and medium sedan by Han et al.[49] and the data obtained in Svoboda and Šolc.[14] for a child against a Skoda Fabia vehicle, with a very good concordance.

In Han et al. four different types of vehicle are investigated by finite element method (FEM) simulations, using a human model of 50th percentile and another with a 1.65 m height and mass of 60 kg that is found in a lateral position with respect to the vehicle. [49] Figure 9(b) shows the comparison between SUV and sedan values obtained in Virzi Mariotti and Golfo,[1] considering only the condition of the pedestrian in the frontal position, with the vehicle braking and at constant speed; one can note that the condition of braking is less dangerous for the pedestrian. The results of the SUV and sedan with the 60 kg dummy are only used for the comparison in Figure 9(c). One can note the SUV data

Figure 5. Frontal Impact at constant speed 20 km/h. The sequence from the beginning of the impact until the end is shown in seven time intervals.

are somewhat lower than the previous sedan data; this is due to the fact that the SUV's frontal shape sets the injuries to the chest and head. This circumstance was noted also for the teenage cyclist in Carollo et al.,[52] also if the SUV has a different manufacturer, but similar front shape. The data presented in Han et al. confirms this evaluation, even if the dummy has a greater mass (difference of 15 kg) and a greater height than the teenager dummy.[49] Any difference can be attributed to this circumstance and to the fact that the vehicles have

different mass and different front shapes. Of course the circumstances described cannot have a general validity, since the result may be influenced by other factors such as unevenness of the vehicle frontal part, so that the result has validity for the examined SUV only. To obtain a general result, other simulations have to be designed with other SUVs having different frontal shapes. The previous observations are confirmed, with the difference that the advantage of the braking is not as marked as in the case of frontal position. However,
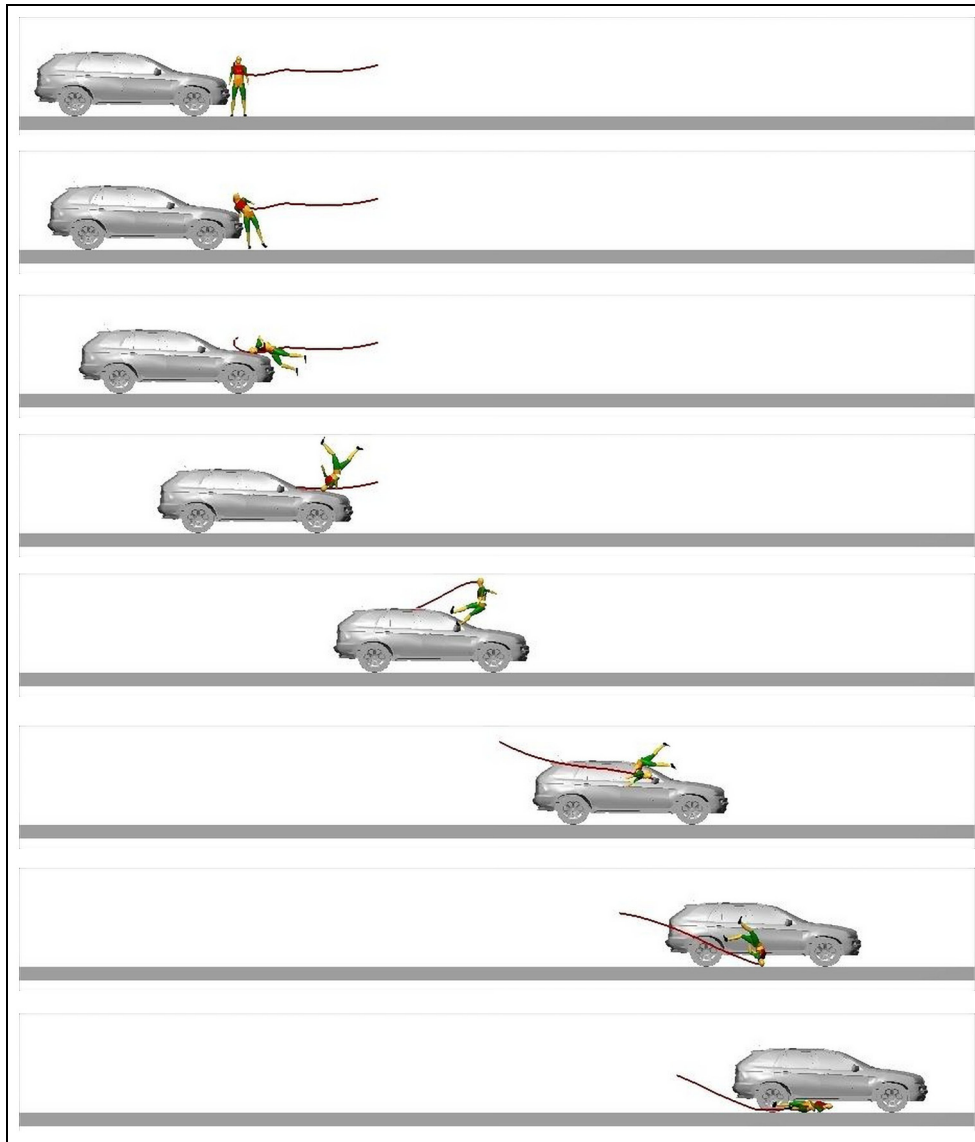
Figure 6. Lateral impact at constant speed 50 km/h. The sequence from the beginning of the impact until the end is shown in eight time intervals.

the lateral position is less dangerous than the frontal, in all the circumstances.

One can note that the frontal shape has a very great significance in the injury to the pedestrian's head (or chest). In the work on the teenage cyclist–vehicle impact[52] the fundamental parameters such as: bonnet angle, bonnet height and bumper height are individuated; Figure 2 shows these parameters and their value for the SUV of this work. Table 3 compares the values with those of the sedan in Virzi Mariotti and Golfo.[1]

TTI calculation

As per the rules, TTI is calculated by means of the relationship

$$TTI = 1,4AGE + 0,5(RIBy + T12y)m_c/Mstd \qquad (2)$$

Teenager age is indicated by AGE (equal to 15 years), his mass m_c is 45 kg, Mstd is the standard mass equal to 75 kg, RIBy [g] represents the maximum of the absolute value of the lateral acceleration of the fourth or eighth rib, on the side it is affected; T12y [g] indicates the absolute value of the maximum lateral acceleration of the 12th thoracic vertebra; both are expressed as multiples of gravity acceleration. Some modifications are reported to the anthropomorphic model to measure the last two quantities. These modifications are listed and described in detail in a previous paper;[1] this allows the insertion of virtual accelerometers for obtaining the values of the 4th rib and 12th vertebra. The last are reported in Table 4 in the cases of lateral impact at constant speed and with braking. In general, braking of the vehicle increases the duration of the peak acceleration, but this consideration has no significant influence in TTI cases, since this method analyses the accelerations, but not their duration.

TTI values can be compared with other data in the literature.[1] Table 5 shows the TTI values calculated by
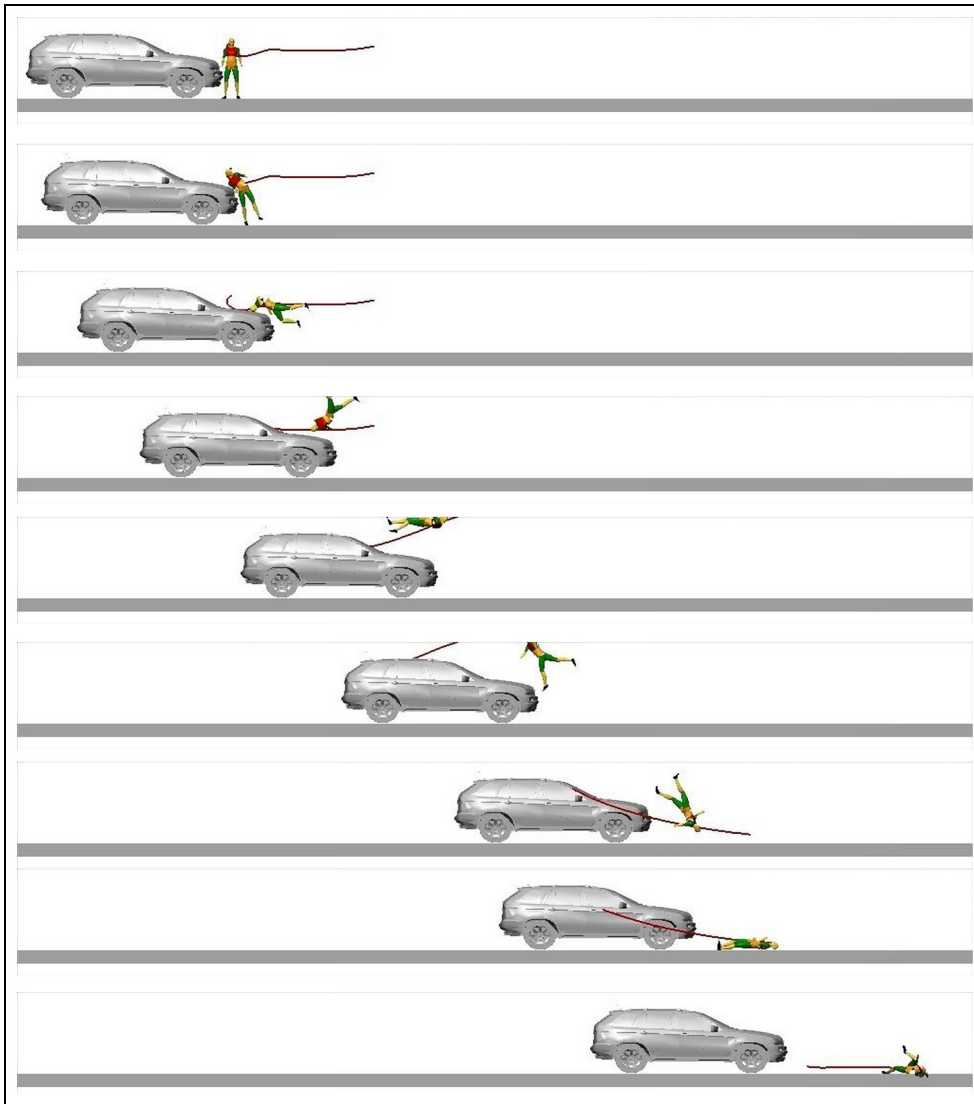
Figure 7. Lateral impact at 50 km/h with braking. The sequence from the beginning of the impact until the end is shown in nine time intervals.

relationship 2, the comparison with sedan results and the percentage difference.

A further comparison of TTI values can be made with other available data in the literature. Previous papers[13,14] contain analysis of the vehicle–pedestrian impact; the simulations are executed by means of the software SIMPACK and MAYDMO, respectively. MADYMO simulations are executed using a Skoda Fabia vehicle against an adult or child pedestrian; values at speed 10 km/h are also determined. The results for the child are shown in Figure 10, with the teenager results in Table 4. SIMPACK results are not used because they are related to an adult. Figure 10 shows that the thorax injury does not differ significantly between the conditions of constant speed and braking. Moreover, the modifications on the dummy are essential and functional. The SUV vehicle causes a lower injury in the thorax than the sedan in Virzi Mariotti and Golfo, [1] and the sedan in Svoboda and Šolc,[14] despite the greater mass. Variation is very strong at 40

km/h; however, the difference depends on the contact point, the shape of the front vehicle, and on the difference in mass. Other results are very close.

TTI–AIS correlation

A correlation scale exists between TTI value and AIS code. The trend in literature shows the lack of values with reference to AIS1+ and AIS2+, because there is surely no probability of death for such injury indices. Virzi Mariotti and Golfo [1] shows that impact with a sedan at a speed of 50 km/h gives the probability of injury AIS3+, or pulmonary contusion and multiple fractures to the skeleton; the probability is 40–42% in the case of constant speed and is around 10% in the case of braking.

Considering the values in Table 4 for the SUV vehicle, there are no fatal injuries for speeds between 20 and 50 km/h; in fact, such values are found in a range between AIS1+ and AIS2+, where the injuries to the skeleton and soft tissues are rather limited.

Table 2. HIC values, fatality percentage and comparison with sedan.[1]

Pos.	Speed [km/h]	Conditions	A_{max} head [g]	HIC	AIS	Fatality [%]	HIC Difference Sedan- SUV [%]
Side	20	Braking	24.15	28.55	1	0	−81
	30		47.32	180.98	1	0–5	−69
	40		72.32	538.72	2	5–10	−52
	50		108.19	1246.26	3	40–45	−24
	20	Constant	31.31	46.20	1	0	−51
	30		57.61	297.88	1	0–5	−55
	40		86.30	849.87	2	10–15	−25
	50		114.73	1386.53	4	45–50	−7
Front	20	Braking	38.96	124.57	1	0	−47
	30		77.95	485.81	1	0–5	−18
	40		100.89	943.92	3	20–25	−6
	50		104.90	1622.55	4	70	−9
	20	Constant	44.47	141.21	1	0	−46
	30		77.30	524.48	2	0–5	−35
	40		120.34	1442.48	4	55–60	18
	50		119.28	1992.48	6	90	19
	20	Mean values for		85.1325			
	30	the several		372.2875			
	40	positions and		943.7475			
	50	conditions		1561.955			

Figure 8. Correlation HIC–AIS; (a) side in braking; (b) side at constant speed.
(c) frontal in braking; (d) frontal at constant speed.

Chest injury by 3 ms criterion

Rules prescribe the use of 3 ms criterion in the case of a frontal impact. The gravity centre of the chest and of the head must not endure greater acceleration than 60 and 80 g respectively for more than 3 ms. A virtual accelerometer is inserted in the chest gravity centre, facilitating the obtaining of results at constant speed and in braking, as Table 6 shows. The last column shows the corresponding probability AIS4+ that is calculated by the following relationship
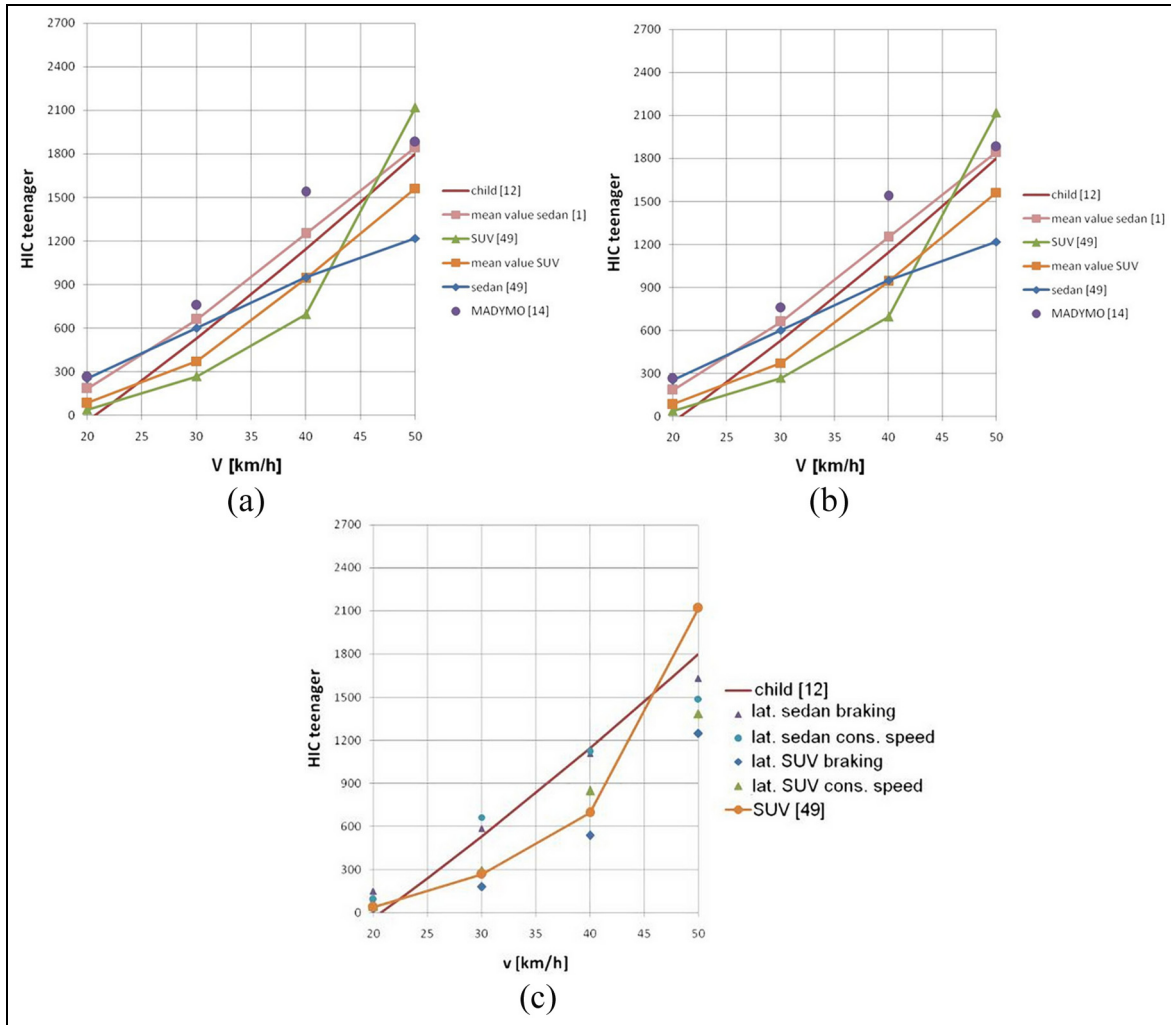
Figure 9. (a) Comparison of sedan and SUV mean values with the literature data; (b) results obtained in pedestrian frontal position; (c) results obtained in pedestrian lateral position.

Table 3. Frontal dimensions of sedan and SUV vehicle.

Vehicle	Bonnet height [mm]	Bumper height [mm]	Bonnet angle [°]	Mass [kg]
Sedan	847	390	20	968
SUV	945	550	15	2270

Table 4. Maximum accelerations to TTI evaluation (side position against SUV).

Speed [km/h]	Conditions	Acc. 4th rib [g]	Acc. 12th vertebra [g]
20	Braking	12.83	13.00
30		41.26	7.40
40		65.84	21.13
50		104.78	71.14
20	Constant speed	13.38	14.94
30		31.97	12.48
40		23.69	62.04
50		86.85	71.14

$$Prob(AIS4 +) = 1/(1 + exp(4,3425 - 0,0630 * gt)$$

(3)

and is equal to 36% for gt = 60 g.

The teenager's chest endures very high accelerations in the case of a frontal impact, which is due to the greater ability of bend that the trunk has, in the direct contact between the chest and the bonnet; it does not occur in the case of lateral impact since the first contact with the bonnet occurs by the shoulder.

Femur injury evaluation

The method used in this paper is the evaluation of the contact maximum force. The collision force during the crash is presented as a bell curve with a big peak. The force-time curve calculation requires the analysis of the structural deformation during the crash. The area subtended by this curve is named the collision impulse; the maximum collision force depends on the peak amplitude. Given that SimWise simulates the body motion in the hypothesis of perfect stiffness, the collision may be
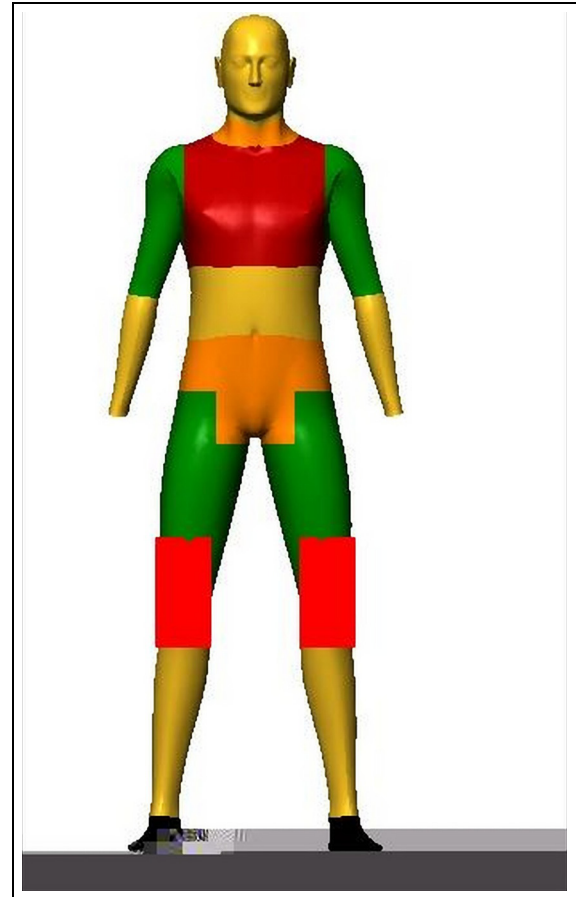
Table 5. TTI values and comparison.

Speed [km/h]	Conditions	TTI SUV [g]	TTI sedan [g]	Difference [%]
20	Constant	29.50	35.50	−17%
30	speed	34.34	41.00	−16%
40		46.72	61.70	−24%
50		72.32	118.00	−39%
20	Braking	28.76	31.50	−9%
30		35.60	40.40	−12%
40		47.10	63.00	−25%
50		73.78	102.00	−28%
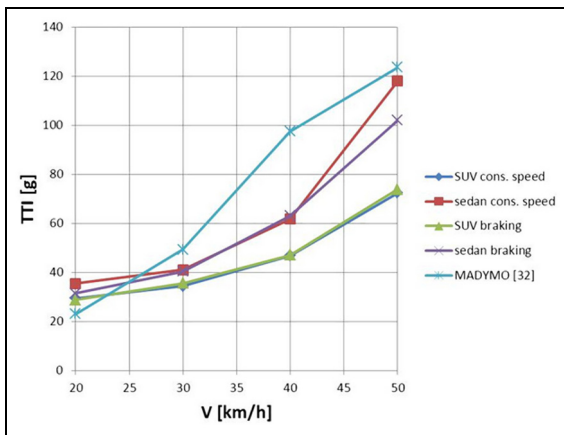
Figure 10. TTI values for the different simulations (child and teenager).

Figure 11. Insertion of the bodies (in red).

considered almost immediate. SimWise offers the possibility of choice between two different contact models; the default model is named "Impulse/Momentum."

Problems regarding the impulse measurement occur during the simulations campaign, due to the contact point uncertainty in the femur, since the vehicle front shows unevenness; this problem is resolved by inserting in the dummy two bodies having rectangular shapes, connected to the thigh and knee by the constraint "rigid joint," with a small thickness and sufficient size to cover the space where the contact presumably occurs; moreover they are linked to a temporal constraint that undoes the use and the functionality, as soon as the contact impulse occurs; this way, the impact dynamics are not modified. Figure 11 shows the positioning of such elements, while Figure 12 shows their separation.

Simulation results. Impulse values and the relative duration are obtained by the method of "contact impulse" for both the conditions of frontal and side impact. Data relating to both the femurs are measured for the frontal impact, while only the data relating to the femur subjected to the impact are measured in the side impact. Figure 13(a) shows the graphs in the frontal impact at a constant speed of 20 km/h. Figure 13(b) shows the side impact graph at the constant speed 30 km/h.

Table 6. 3 ms criterion results (frontal impact against SUV).

Speed [km/h]	Conditions	3 ms [g]	Prob. (AIS 4+)
20	Braking	29.75	7%
30		54.62	28%
40		80.40	67%
50		109.58	92%
20	Constant speed	39.50	13%
30		61.72	38%
40		127.21	97%
50		140.89	98%

Tables 7 and 8 show the results for all the simulations. As the force is the derivative of the impulse, and the trend is linear, the force value is obtained dividing the impulse maximum value by the elapsed time between zero and the maximum.

One can note that the right femur is most damaged in all the simulations, due to the dummy not being in a perfectly centred position, as in a real case, so that one femur endures a greater force. Instead, in the lateral impact, the extrapolation data are related to the femur that comes into contact with the vehicle. For this reason, there is very small difference in the results.
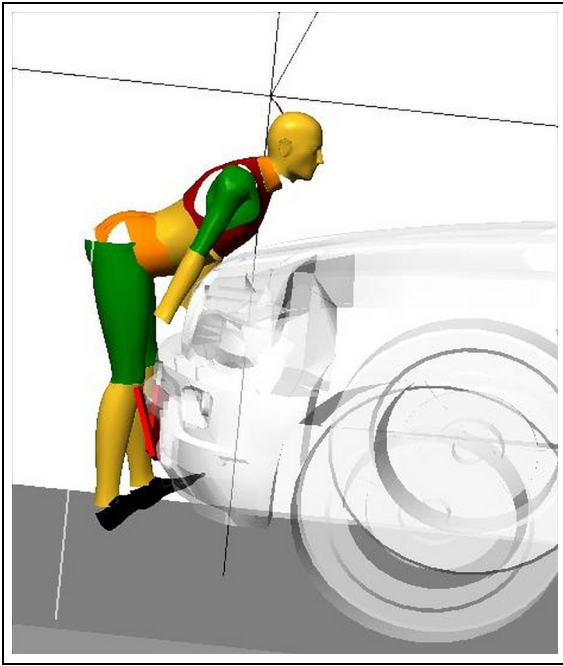
Figure 12. Separation after the collision.

The values of the femur contact force may be compared with similar data available in the literature. Schejbalová et al.[45] studied the vehicle–pedestrian impact analysis, executed by a dummy P6 (m 1.17, 22 kg) in frontal position in relation to the vehicle, with adequate instrumentation for impact force evaluation at a speed of 10-20-30 km/h; the vehicle was Skoda Octavia having a mass of 1255 kg. The datum at 40 km/h was obtained from DeSantis Klinich;[59] the values are shown in Table 6, and Figure 14 shows the visual comparison; one can note the very good concordance between the data. The last column of Table 6 shows the discrepancy in percentage.

The comparison shows that the approximation and the modifications on the dummy for the femur contact force measurement are indispensable and functional, and they do not distort the result. The discrepancies are acceptable at all the speeds and authors did not find data for the speed of 50 km/h.

Knee bending criterion for the dummy (Hybrid III) and FEM leg form impactor are applied in a previously published paper[60] for the adult pedestrian–SUV impact.

Contact force–AIS correlation. A correlation scale exists between the femur force value and the corresponding AIS code. Figure 15 shows the trend,[36] by referring to the code AIS $2+$ corresponding to the femur fracture, or the pelvis fracture or the knee break with its ligaments. Figure 15 shows also the risk value for the right femur of the pedestrian in a frontal position. Table 9 summarizes the probability of the pedestrian enduring an AIS2+ code versus the variation of speed and position. The risk of femur break increases with the speed
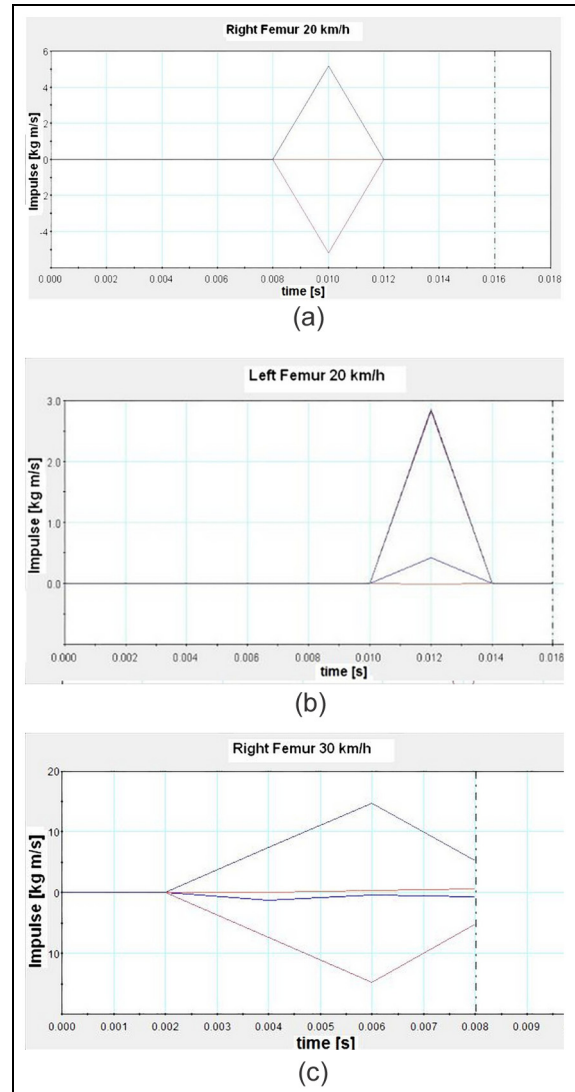
Figure 13. Impulse in the frontal impact at a constant speed of 20 km/h. (a) right femur; (b) left femur. Impulse in the side impact at a constant speed of 30 km/h (c) right femur.

and assumes considerable value at the speeds of 40 and 50 km/h, according to the literature data.

Impact points localization

Figures 16 and 17 show the bonnet areas most often involved in the head impact with the vehicle frontal part. The vehicle marking of the areas wrap around distance (WAD) is done following the EURONCAP rules. In particular, the impact points are marked with several indicated speeds; one can read:

- in *red*, the impact points for the frontal impact with vehicle at constant speed;
- in *green*, the impact points for the frontal impact with vehicle in braking;
- in *blue*, the impact points for the side impact with vehicle in braking; and

Table 7. Results in the case of frontal impact against the SUV.

Speed [km/h]	Right femur		Left femur		Force [kN]			Discrepancy left–right [%]
	Impulse [kg m/s]	Time [ms]	Impulse [kg m/s]	Time [ms]	right	left	Exp.[45,59]	
10	3.75	1.86	1.06	1.80	2.01	0.56	0.877	39
20	5.21	2.00	2.85	2.00	2.6	1.40	2.497	2
30	7.82	2.00	16.90	6.00	3.91	2.81	3.41	7
40	12.20	2.00	14.80	4.00	6.10	3.70	5.5	12
50	35.86	4.00	28.00	6.00	8.91	4.66		

Table 8. Results in the case of side impact against the SUV.

Speed [km/h]	Right femur		Force [kN]
	Impulse [kg m/s]	Time [ms]	
10	6.53	4.00	1.61
20	10.20	4.00	2.55
30	14.70	4.00	3.67
40	25.30	4.00	6.32
50	35.30	4.00	8.83

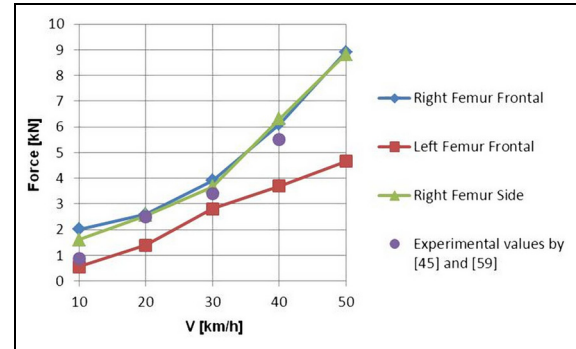**Figure 14.** Contact force on the femur versus the speed.

- in *violet*, the impact points for the side impact with vehicle at constant speed.

Impact point dispersion is localized in both the cases in the zone between WAD 1000 and WAD 1500. While the impacts at 20 and 30 km/h are found closer to WAD 1000, the others are found closer to WAD 1500.

In general, the greater acceleration peaks correspond to an impact against a more rigid part of the vehicle front. The impact point position is different in the case of a SUV and the sedan. In the case of the SUV, all the contact points fall between WAD 1000 and WAD 1500. In the case of the sedan, the teenage pedestrian head hits the upper part of the bonnet always in the zone between WAD 1000 and WAD 1500, but the impact points at 40 km/h are found closer to the windscreen, while the head hits the windscreen at 50 km/h. These differences are due to the differences in the frontal parts of the vehicle and the height of the parts in relation to the pedestrian.

A theoretical approach to pedestrian–vehicle impact on speed evaluation

The speed data obtained are analysed by means of the theoretical results given by the momentum and kinetic energy conservation; both can be considered suitable by making the hypothesis of a fully elastic collision. The used parameter is the gravity centre speed of the chest. The values of the speed of the dummy gravity centre should be used in a more correct way, but the difference is very small. Table 10 shows the maximum speed data for both the vehicles. Normalized speed is obtained by dividing the chest speed by the vehicle

speed in coherent unities. Table 11 shows the vehicle speed after the impact obtained by the simulations: the small slowing is due to the loss of a small part of vehicle kinetic energy that is transferred to the pedestrian. Slowing down of the sedan is greater than that of the SUV, due to the difference in mass of the two vehicles.

Carollo et al.[52] shows the theoretical approach for determination of the speed after the collision, and is summarized here: x indicates the motion direction, y and z the transverse and vertical directions respectively, V is the vehicle initial impact speed that has a known value, while the final values V_c (of the pedestrian) and V_v (of the vehicle) are unknown. In general, the six components of speed are different by zero in the final instant. Momentum conservation is

$$
\begin{aligned}
m_c V_{xc} &= -m_v(V_{xv} - V) \\
m_c V_{yc} &= -m_v V_{yv} \\
m_c V_{zc} &= -m_v V_{zv}
\end{aligned}
\tag{4}
$$

Squaring the relationships (4) and summing, remembering

$$
\begin{aligned}
V_c &= \sqrt{V_{xc}^2 + V_{yc}^2 + V_{zc}^2} \\
V_v &= \sqrt{V_{xv}^2 + V_{yv}^2 + V_{zv}^2}
\end{aligned}
\tag{5}
$$

the following relationship is obtained

$$
m_c^2 V_c^2 = m_v^2\left(V_v^2 + V^2 - 2V_{xv}V\right)
\tag{6}
$$

another equation can be obtained by applying the energy conservation principle. One has
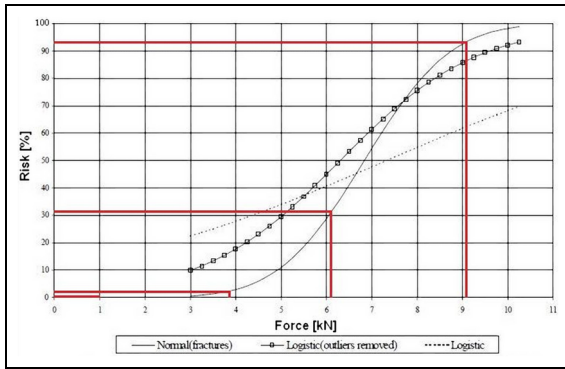
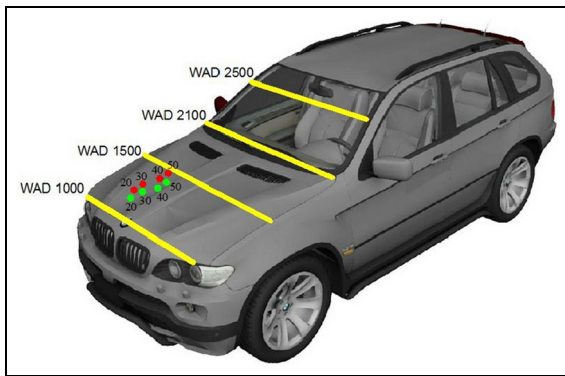**Figure 15.** Contact force–AIS correlation in the frontal impact.

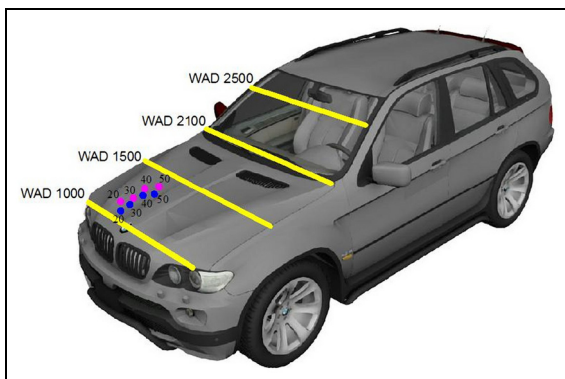**Figure 16.** Frontal impact, contact points vehicle-head The speeds [km/h] are marked.

Figure 17. Side impact; contact points vehicle-head The speeds [km/h] are marked.

$$\frac{1}{2} m_c V_c^2 = -\frac{1}{2} m_v \left(V_v^2 - V^2 \right) \tag{7}$$

The energy conservation principle is written neglecting all the other forms of energy. Introducing the vehicle normalized speed $X = V_v / V$, the pedestrian normalized speed $Y = V_c / V$ and the direction cosine $\beta = V_{xv} / V_v$, relationships (6) and (7) become

$$m_c^2 Y^2 = m_v^2 \left(X^2 + 1 - 2\beta X \right) \tag{8}$$

$$m_c Y^2 = -m_v \left(X^2 - 1 \right) \tag{9}$$

Table 9. Probability of AIS2+ injury.

Right femur in frontal position		Right femur in side position	
Speed [km/h]	AIS 2+ [%]	Speed [km/h]	AIS2+ [%]
10	0	10	0
20	0	20	0
30	2	30	2
40	31	40	34
50	93	50	91

Relationships (8) and (9) form a system of two equations in three unknowns X, Y and β. The system can be resolved in a conditioned way by making use of Lagrange multipliers λ.[61] The solution is

$$X_0 = \pm \sqrt{\frac{m_v - m_c}{m_v + m_c}} \quad Y_0 = \pm \sqrt{\frac{2m_v}{m_v + m_c}} \quad \beta = \pm \sqrt{1 - \frac{m_c^2}{m_v^2}} \tag{10}$$

Some specific cases are indicated in Carollo et al.[52] Here β and X_0 have the same sign, while the case $Y_0 < 0$ has no interest in the examined case. The solution has to be reconsidered in the case $m_c > m_v$; however, this case too is not interesting for the purpose of this work. In general relationships (4) allows the reconstruction of the speed of both the body, if the motion is supposed in the plane x-z.

Substantially, the procedure allows calculation of the results, so that the solutions of the system constituted by (8) and (9) are real and in agreement. From the geometrical view point,[61] it yields curves represented by the above relationships, tangent in the point (X_0, Y_0) in the X-Y plane.

The second relationship (10) shows that the speed of the pedestrian can be greater than the vehicle impact speed, since the normalized speed tends to 1.41 if $m_c << m_v$. However, the vehicle mass effect is greater as soon as the impact speed V increases.

Tables 9 and 10 show the normalized impact speed for both the sedan[1] and SUV. One can note that the normalized speed X always assumes a few lower values than 1 and that the cyclist's speed after the impact is greater than the vehicle impact speed. The normalized speed Y assumes values between 1,2 and around 2, against the collision theoretical value 1.41 above indicated. This is due to non-fully elastic collision, and to the fact that the energy conservation (7) does not take in account other energy forms. Table 12 shows the mass and β value for both the vehicles.

β values are very near to one, given that the vehicle mass is much greater than that of the pedestrian, but one has to highlight that rounding up distorts the result. Figure 18 shows the comparison between the simulations and theoretical results in the X-Y plane. Of course the values in braking are not taken into account, because the slowing is due also to the braking. The relationships (8) and (9) are tangent to one another, while

Table 10. Speed values obtained by the simulations.

Vehicle speed [km/h]	Pos.	SUV		Sedan[1]	
		Chest speed [m/s]	Normalized chest speed	Chest speed [m/s]	Normalized chest speed
20	F	8.43	1.5174	9.74	1.7532
30	F	12.165	1.4598	13.26	1.5912
40	F	15.06	1.3554	15.07	1.3563
50	F	17.64	1.27008	18.5	1.332
20	S	9.99	1.7982	7.09	1.2762
30	S	12.57	1.5084	12.34	1.4808
40	S	16.73	1.5057	15.16	1.3644
50	S	17.38	1.25136	18.14	1.2427

Table 11. Slowing down and normalized speed of the vehicle.

Vehicle speed [km/h]	Pos.	SUV			Sedan[1]		
		Post impact vehicle speed [m/s]	Slowing [km/h]	Norm. post impact speed	Post impact vehicle speed [m/s]	Slowing [km/h]	Norm. post impact speed
20	F	5.427	0.4628	0.97686	5.11	1.604	0.9198
30	F	8.155	0.642	0.9786	7.89	1.596	0.9468
40	F	10.906	0.7384	0.98154	10.55	2.02	0.9495
50	F	13.665	0.806	0.98388	13.26	2.264	0.95472
20	S	5.374	0.6536	0.96732	5.26	1.064	0.9468
30	S	8.143	0.6852	0.97716	7.98	1.272	0.9576
40	S	10.858	0.9112	0.97722	10.56	1.984	0.9504
50	S	13.671	0.7844	0.984312	13.39	1.796	0.96408

Table 12. Masses and directional cosine for the pedestrian and the cyclist.

	Mass [kg]	β		Mass [kg]	β
Pedestrian	45		Cyclist	45	
Sedan[1]	968	0.9989188	Sedan	968	0.998919
SUV	2270	0.9998034	SUV	2900	0.99988
			Pick Up	3085	0.999894

the values obtained by the numerical simulations are shown through superimposition. The values obtained are in perfect good agreement with theoretical ones. The figure shows that:

- All the simulation data are very close to the optimum condition obtained in the previous study;
- Pedestrian speed at the end of the contact is significantly higher than the speed of the vehicle coming up (up to two times); and
- SUV behaves better than the sedan, since its values are very closer to the optimal condition (X_0, Y_0).

The following procedure is useful to highlight that the mass influence: relationships (10) suggest the following coordinate transform

$$Y = Y'\sqrt{\frac{2m_v}{m_v + m_c}} \quad X = X'\sqrt{\frac{m_v - m_c}{m_v + m_c}} \quad (11)$$

This way, the tangency point of the previous study has coordinates $(X_0' = 1, \ Y_0' = 1)$ for whatever vehicle. Substituting (11) in relationship (9), the derivative in the point (1,1) is

$$\frac{dY'}{dX'}(1, 1) = a = -\frac{m_v - m_c}{2m_c} = -\frac{1}{2}\left(\frac{m_v}{m_c} - 1\right) \quad (12)$$

The tangent equation at both the kinetic and momentum curves in the point (1,1) can be constructed.

Carollo et al. show the results of analogous simulations of the impact of a teenage cyclist with a vehicle.[52] Table 12 shows the mass and the directional cosines, with analogous observation on the β calculation. The tangents are drawn in Figure 19; their slope a is strongly dependent on the vehicle mass (m_v/m_c ratio). All the data of vehicle and of pedestrian normalized speeds, in Tables 9 and 10, are converted by using the relationships (11). The corresponding points are shown in Figure 19. The simulation results are thickened around
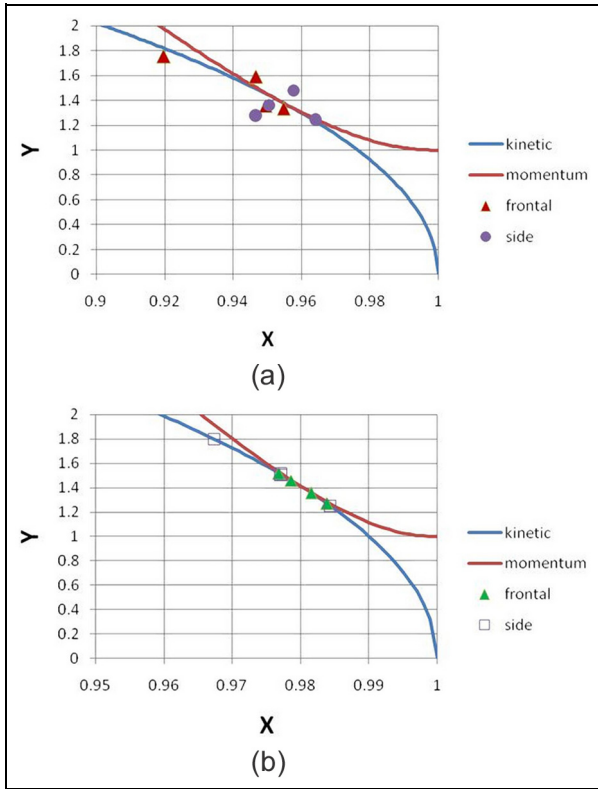
Figure 18. Comparison between numerical and theoretical values for the sedan (a) and SUV (b).
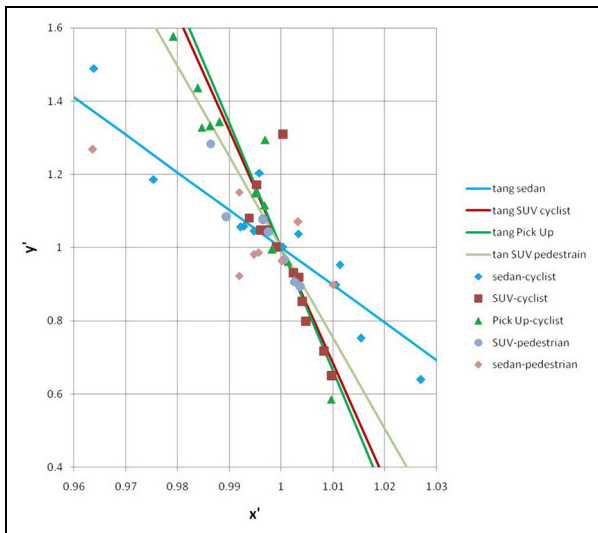
Figure 19. Comparison among the different simulations for teenage pedestrian and cyclist impact.

the point (1,1) and are positioned around the tangent line having slope *a* (12). The figure confirms the excellent concordance of the theoretical result with the numerical simulation.

Many papers are found in the literature that indicate that the impact velocity of the head or chest is very close to the speed of the vehicle. This result can only be achieved considering a fully inelastic collision; the FEM
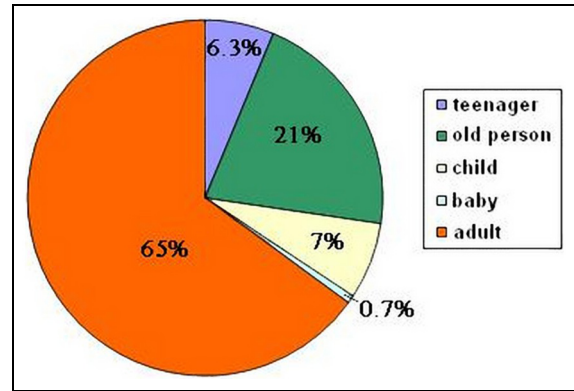
Figure 20. Distribution of incident casualty vehicle–pedestrian by age group.

mesh is limited to the front of the vehicle, considering the stiffness of the parts, but no indication is given as to the mass value; this probably makes possible the careful evaluation of the influence of vehicle front shape, but does not allow for a proper evaluation of the kinematics of the parts, given that a vehicle slowing has to be present also in the case of fully inelastic collision, due to conversion of kinetic energy. However, this circumstance may have little influence on TTI and HIC values, but is a possible offshoot of this work; the application of the fully elastic condition parameters is a normal custom in the forensics room.

The results of this work show that the pedestrian speed, with his body parts, assumes values that are strongly dependent on the vehicle mass. Results can be improved by increasing the number of vehicles examined, and also considering the offset of impact in the lateral crash. They may be used as the starting data for the mathematical procedures that can lead to improving the result.

Comparison of the theoretical and numerical results shows that the theory has excellent validity in the case of a teenage pedestrian or cyclist crash, and can find application in other impact conditions.

Result validation by accident data

A series of accident data in Palermo and province in the last three years were collected to validate the chosen solution and the conclusions obtained. The data was provided by four insurance companies and covers a total number of 3141 vehicle accidents in the period indicated. Of these, 271 concern pedestrian–car accidents, while 70 concern car–cyclist accidents. Figure 20 shows the accidents between pedestrians and cars: one can note that the teenager accidents amount to 6.3% of the examined cases, while adult pedestrians account for 65% and children 7%. The data on adult pedestrian or children are easily found in literature, while teenager data are found with difficulty; this validates the choice of the teenager in this and previous papers. Figure 21
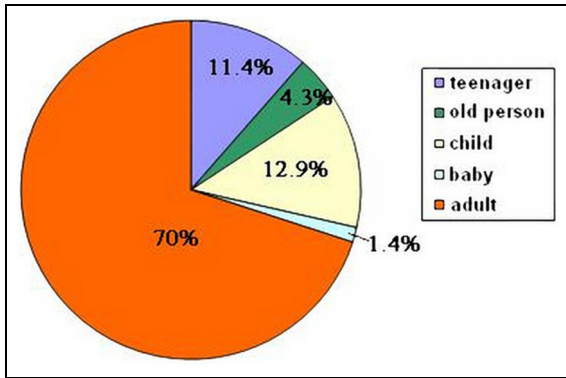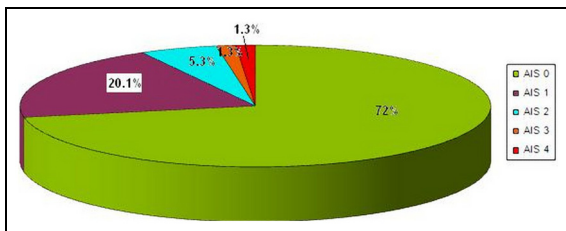
Figure 21. Distribution of incident casualty vehicle–cyclist by age group.
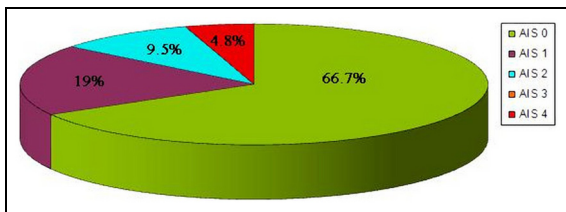
Figure 22. Distribution of front and rear impacts of the head region on the AIS scale (value AIS3 = 0 is obtained).
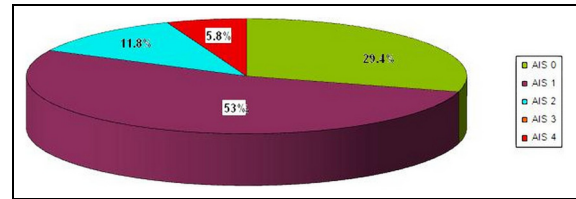

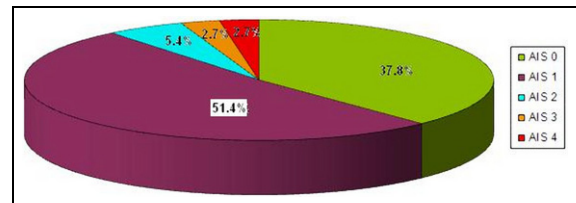**Figure 23.** Distribution of side impacts of the head region on the AIS scale.

Figure 24. Distribution of front and rear impacts of the thorax region on the AIS scale (value AIS3 = 0 is obtained).

Figure 25. Distribution of side impacts of the thorax region on the AIS scale.

in the side crash; the value AIS = 0 is obtained in 72% of the accidents, while the other percentages are lower (except AIS = 3) than the previous case.

Figure 24 shows the result for the thorax of the pedestrian in a frontal crash. The selection does not indicate results for AIS = 3, while the value AIS = 0 is obtained in 29.4% of the accidents and the value AIS = 1 is obtained in 53% of the cases. Figure 25 shows the results for the thorax in the side crash; the value AIS = 0 is obtained in 37.8% of the accidents, while the value AIS = 1 is obtained in 51.4% of the cases. Of course the percentage of higher AIS is lower in the case of side impact.

The analysis of the accident data confirms the simulation result: in general, the lateral crash is less dangerous for the pedestrian or the cyclist than the frontal impact.

shows that analogous observation can be performed for the vehicle–cyclist impact.

Moreover, the data are examined in order to assign an AIS value for every single accident, for the head and the thorax only, following the tables reported in previously published papers[29],[33]; in addition, the selection of the side or frontal position is performed for each accident. A total of 38 cases of frontal crash for the head and thorax were examined, while 112 cases were examined for side crash. It confirms that the accidents in the frontal position are about 30% of the cases of side impact. (40% of the total). In addition, numerous double cases and impact with legs are found.

Figure 22 shows the result for the head of the pedestrian or cyclist in a frontal crash. The selection does not give results for AIS = 3, while the value AIS = 0 is obtained in 66.7% of the accidents. Figure 23 shows the results for the head of the pedestrian or the cyclist

Conclusions

The objectives of this work were the evaluation of the injury to the teenage pedestrian during impact with a SUV, analysis of the possible dynamics and thereby making a contribution to the improvement of safety conditions.

Comparison with other experimental or numerical literature data indicates a series of possible considerations: the pedestrian's height, the shape of the vehicle frontal part, the vehicle's minimum height from the ground, the height of the bumper and the bonnet inclination are extremely important factors for the impact fatality. In Virzi Mariotti and Golfo,[1] the teenager limits the contact points of the head to the sedan bonnet or the lower part of the windscreen, while the teenager's head hits the SUV on the bonnet lower part only. This is an advantage, since the bonnet has

certainly a lower inclination and less stiff structure than the windscreen, so that the teenager faces a lower probability of a fatal impact. The SUV's frontal part does not have much of an acute trend, and has a larger and higher vertical profile than the sedan, with some asperity. This does not limit the contact point concentration force during the impact (very dangerous conditions for the legs), in spite of the pedestrian rotation on the bonnet, reducing speeds and accelerations. In fact the parameters (HIC, TTI, 3 ms) have lower values.

The analysis confirms that the frontal position is more dangerous than the lateral one, because the contact of the head and the chest occurs on the bonnet directly, while the pedestrian in side position hits the bonnet with the shoulder; this limits the injuries to the fatal parts; this circumstance is confirmed by the analysis of accident data this confirms the opportunity to sensitize people on this subject. On the contrary, the lesion in the femur does not undergo great variations with the position.

A multibody model has a series of advantages, for example, the designers of a vehicle manufacturing house have the possibility to execute the simulations when the prototype CAD model exists, so that one may study the vehicle's aggressiveness, to pass the mandatory homologation tests in relation to the pedestrian, avoiding the FEM mesh. Designers can make more opportune and esthetic functional changes, testing the vehicle in a fast and economic way. The same can be true of the dummy: measurement problems of TTI are resolved by inserting virtual accelerometers to obtain the acceleration values of the 4th rib and 12th vertebra; the measurement problems of the femur force are due to the fact that the precise positioning of the contact point depends on the pedestrian's height and the bumper position; they are resolved by inserting in the dummy two bodies having a rectangular shape, connected to the thigh and knee, having sufficient size to cover the space where there is a possible point of contact. This allows the force measurement and the evaluation of the leg injury in an accurate way.

The speed results of the simulations are compared with an original theoretical procedure, based on the application of momentum and energy conservation principle in the hypothesis of a fully elastic collision. The results show that the system teenage pedestrian–vehicle naturally assumes a speed condition that can be calculated with simplicity. Result analysis indicates that the pedestrian (or cyclist) assumes a speed that can be much higher than that of the vehicle coming up; this results in the vehicle slowing and a small component of the vehicle speed along the orthogonal plane to the motion, due to a value of the directional cosine a few lower than 1.

The same theoretical procedure shows that the vehicle mass has non-negligible importance and that the collision with the pedestrian leads to a slowing down due to a part of the vehicle kinetic energy being transferred to the pedestrian; the slowing increases with the reduction of the vehicle mass; research on this scope are not found in the literature, except in Carollo et al.[52]

The effectiveness of active and passive devices can be tested through the simulations; for example, to evaluate the performances of soft bumpers, or the bonnet angle, which are the only devices of active protection introduced up until now. In conclusion, system applications can be studied as part of accident dynamics in the forensics room.

Declaration of conflicting interests

Funding

References

1. Virzi' Mariotti G and Golfo S. Determination and analysis of the head and chest parameters by simulation of a vehicle–teenager impact. *Proc IMechE Part D: J Automobile Engineering* 2014; 228: 3–20.
2. Williams AF and Tison J. Motor vehicle fatal crash profiles of 13–15-year-olds. *J Safety Res* 2012; 43; 145–149.
3. Bellavia G and Virzi' Mariotti G. Multibody numerical simulation for vehicle–pedestrian crash test. In: *Ingegneria dell'autoveicolo ATA, vol. 62, XXI science and motor vehicles 2007, JUMV international conference with exhibition*, Belgrade, Serbia, 23–24 April 2007, pp.40–49. Torino: JUMV.
4. Bellavia G and Virzi' Mariotti G. Development of an anthropomorphic model for vehicle–pedestrian crash test. In: *Ingegneria dell'autoveicolo, vol. 62, XXI science and motor vehicles 2007, JUMV international conference with exhibition*, Belgrade, Serbia, 23–24 April 2007, pp.48–56. Torino: JUMV.
5. Kleinberger M, Sun E, Eppinger R, et al. *Development of improved injury criteria for the assessment of advanced automotive restraint systems*. Washington, DC: National Highway Traffic Safety Administration, 1998.
6. Chaurand N and Delhomme P. Cyclists and drivers in road interactions: a comparison of perceived crash risk. *Accid Anal Prev* 2013; 50: 1176–1184.
7. Detweiler DT and Miller RA. Development of a sport utility front bumper system for pedestrian safety and 5 mph impact performance. In: *Proceedings of the 17th international technical conference on the enhanced safety of vehicles*, Amsterdam, 4–7 June 2001, Paper Number 01-S6-W-145. Washington, DC, USA: National Highway Traffic Safety Administration.
8. Simms CK and Wood DP. Pedestrian risk from cars and sport utility vehicles–a comparative analytical study. *Proc IMechE Part D: J Automobile Engineering* 2006; 220: 1085–1100.
9. Wood DP, Simms CK and Walsh DG. Vehicle–pedestrian collisions: validated models for pedestrian impact

and projection. *Proc IMechE Part D: J Automobile Engineering* 2005; 219: 183–195.

10. Şoica A and Lache S. Theoretical and experimental approaches to motor vehicle–pedestrian collision. In: *3rd WSEAS international conference on applied and theoretical mechanics*. Spain, 14–16 December 2007, pp.263–268. WSEAS Press.

11. Iozsa MD, Micu DA, Cornelia S, et al. Analytical estimation of the Hood behaviour during an impact with a pedestrian head. In: *WSEAS International Conference Recent advances in civil engineering and mechanics*. ISBN: 978-960-474-403-9, pp.195–198.

12. Yang J, Yao J and Otte D. Correlation of different impact conditions to the injury severity of pedestrians in real world accidents. In: *19th international technical conference on the enhanced safety of vehicles*, Washington, DC, USA, 6–9 June 2005, paper number 05–0352. Washington, DC: National Highway Traffic Safety Administration.

13. Kovanda J, Kovandová H and Ságl R. Vehicle–pedestrian collision, simulation in SIMPACK. In: *SIMPACK user meeting 2001*, Bad Ischl, Rakousko, Austria, 2001. Gilching: SIMPACK, http://www.simpack.com/filead min/simpack/doc/usermeeting01/um01-prof_kovanda.pdf

14. Svoboda J and Šolc Z. *Pedestrian protection-pedestrian in collision with personal car*. Report, Prague, Czech Republic: Faculty of Mechanical Engineering, Department of Automotive and Aerospace Engineering, Czech Technical University in Prague, 2001. http://docplayer.net/8398068-Pedestrian-protection-pedestrian-in-collision-with-personal-car.html

15. Wang SC, Qian YB and Qu XG. Reconstruction of car-electric bicycle side collision based on PC-crash. *J Transp Technol* 2014; 4: 355–364. http://dx.doi.org/10.4236/jtts.2014.44032

16. Milne G, Deck C, Bourdet N, et al. In: *2013 IRCOBI conference proceedings - international research council on the biomechanics of injury*. Gothenburg, Sweden, pp.735–746. Zurich, Switzerland: IRCOBI.

17. Kim JK, Kim SP, Ulfarsson GF, et al. Bicyclist injury severities in bicycle–motor vehicle accidents. *Accid Anal Prev* 2007; 39: 238–251.

18. Van Schijndel M, De Hair S, Rodarius C, et al. Cyclist kinematics in car impacts reconstructed in simulations and full scale testing with Polar dummy. In: *Proceedings of the international research council on biomechanics of injury (IRCOBI) conference*, Dublin, 2012, pp.800–812. Zurich, Switzerland: IRCOBI.

19. Fredriksson R and Rosén E. Priorities for Bicyclist Protection in Car Impacts – a Real life Study of Severe Injuries and Car Sources. In: *Proceedings of the international research council on biomechanics of injury (IRCOBI) conference*, Dublin, Ireland, 2012, pp.779–786. Zurich, Switzerland: IRCOBI.

20. van Hassel E and de Lange R. *Bicyclist safety in bicycle to car accidents: an inventory study*. TNO report 06.OR.SA.031.1/RDL, Delft: TNO Automotive, 17 August 2006.

21. Mukherjee S, Chawla A, Mohan D, et al. Effect of vehicle design on head injury severity and throw distance variations in bicycle crashes. In: *Proceedings of 20th international technical conference on the enhanced safety of vehicles*, Lyon, 2007, Washington, DC: National Highway Traffic Safety Administration.

22. Watson JW. *Investigation of cyclist and pedestrian impacts with motor vehicles using experimentation and simulation*. PhD Thesis, Cranfield University, UK, 2010.

23. Peng Y, Chen Y, Yang J, et al. A study of pedestrian and bicyclist exposure to head injury in passenger car collisions based on accident data and simulations. *Safety Sci* 2012; 50: 1749–1759.

24. Chen Q, Chen Y, Bostrom O, et al. A comparison study of car-to-pedestrian and car-to-E-bike accidents: data source: the China in-depth accident study (CIDAS). SAE paper 2014-01-0519, 2014.

25. Maki T, Kajzer J, Mizuno K, et al. Comparative analysis of vehicle–bicyclist and vehicle–pedestrian accidents in Japan. *Accid Anal Prev* 2003; 35: 927–940.

26. Fanta O, Jelen K and Purš H. Interaction between cyclist and car during broadside and confrontation with pedestrian throw formulas multibody simulation. *Trans Transport Sci* 2010; 3: 99–106.

27. Katsuhara T, Miyazaki H, Kitagawa Y, et al. Impact kinematics of cyclist and head injury mechanism in car-to-bicycle collision. In: *Proceedings IRCOBI conference 2014*, Berlin, Germany, 2014, pp.670–684. IRCOBI.

28. Carollo F, Virzi' Mariotti G and Scalici E. Injury evaluation in teenage cyclist-vehicle crash by multibody simulation. *WSEAS Trans Bio Biomed* 2014; 11: 203–217.

29. Carollo F, Virzi' Mariotti G and Scalici E. Biomechanics parameters in the vehicle-cyclist crash with accident analysis in palermo. In: *Recent advances in mechanical engineering, WSEAS international conference ECME'14*, Firenze, 22–24 November 2014, pp.139–148.

30. Carollo F. *Analisi di alcuni parametri biomeccanici nello studio d'impatto auto bici*. Graduate Thesis, University of Palermo, Italy, 2014.

31. Carollo F, Virzi' Mariotti G and Naso V. Biomechanics parameters in teenage cyclist – SUV accident and comparison with the pedestrian. In: *WSEAS-NAUN conference OTENG'15*, Rome, 7–9 November 2015, pp.77–87. Applied Mathematics and Materials.

32. Carollo F, Virzi' Mariotti G and Naso V. HIC evaluation in teenage cyclist–SUV accident. In: *Recent researches in mechanical and transportation systems, WSEAS international conference ICAT'15*, Salerno, Italy, 27–29 June 2015, pp.252–259.

33. Carollo F, Virzì Mariotti G and Scalici E. Valutazione delle lesioni nell'impatto ciclista adolescente - veicolo con simulazione multibody. *Scienze e Ricerche* 2016; 24: 75–88.

34. Carollo F, Naso V and Virzi'Mariotti G. Injury and throwing distance in teenage cyclist-vehicle crash. *WSEAS Trans Power Syst* 2016; 11: 171–182.

35. Neilson ID. Vehicle safety—a review for 1993. *Proc IMechE Part D: J Automobile Engineering* 1993; 207: 117–126.

36. EEVC Working Group. *17 Report, Improved test methods to evaluate pedestrian protection afforded by passenger cars*, December 1998. https://www.unece.org/fileadmin/DAM/trans/doc/2006/wp29grsp/ps-187r1e.pdf

37. Euro NCAP. Assessment Protocol and Biomechanical Limits, Version 4.1. Document, Euro NCAP, Brussels, Belgium, March 2004.

38. Euro NCAP. Assessment Protocol and Pedestrian Testing Protocol, Version 5.3.1. Document, Euro NCAP, Brussels, Belgium, November 2011.

39. Kuppa S. Injury criteria for side impact dummies. NTBRC/NHSTA Document, National Transportation

Biomechanics Research Center, National Highway Traffic Safety Administration, Washington, DC, USA, May 2004.

40. Hamada M, Hasegawa J and Nishimura R. *Application of EEVC upper leg impactor test method to SUVs*: finite element analysis of pedestrian pelvic injuries. *JSAE Trans* 2005; 36: 201–206.

41. Han Y, Yang J, Mizuno K, et al. A study on chest injury mechanism and the effectiveness of a head-form impact test for pedestrian chest protection from vehicle collisions. *Safety Sci* 2012; 50: 1304–1312.

42. Sulzer J, Kamalakkannan SB, Wiechel J, et al. Simplified MADYMO model of the IHRA head-form impactor. SAE paper 2006-01-2349, 2006.

43. Shin MK, Yi SI, Kwon OT, et al. Structural optimization of the automobile frontal structure for pedestrian protection and the low-speed impact test. *Proc IMechE Part D: J Automobile Engineering* 2008; 222: 2373–2387.

44. Carollo F, Naso V and Virzi' Mariotti G. Teenage cyclist: pick up crash by multibody simulation; HIC evaluation and comparison with previous results. *Int J Mech Eng* 2016; 1: 75–83.

45. Schejbalová Z, Kvášová A, Mičunek T, et al. Simulation of a collision between passenger car and child pedestrian. *Safety Security Traffic Prelim Commun* 2012; 24: 109–118.

46. Lee TH, Yoon GH and Choi SB. A shock mitigation of pedestrian-vehicle impact using active hood lift system: deploying time investigation. *Shock and Vibration* 2016; 2016: 17 pp.

47. Lee TH, Yoon GH and Choi SB. Deploying time investigation of automotive active hood lift mechanism with different design parameters of hinge part. *Adv Mech Eng* 2016; 8: 1–16.

48. Liu XJ, Yang JK and Lövsund P. A study of influences of vehicle speed and front structure on pedestrian impact responses using mathematical models. *Traffic Inj Prev* 2010; 3: 31–42.

49. Han Y, Yang J, Mizuno K, et al. Effects of vehicle impact velocity, vehicle front-end shapes on pedestrian injury risk. *Traffic Inj Prev* 2012; 13: 507–518.

50. Li G, Lyons M, Wang B, et al. The influence of passenger car front shape on pedestrian injury risk observed from German in-depth accident data. *Accid Anal Prev* 2017; 101: 11–21.

51. Sankarasubramanian H, Chawla A, Mukherjee S, et al. Optimization study on multibody vehicle-front model for pedestrian safety. *Int J Crashworthines* 2016; 21: 63–78.

52. Carollo F, Naso V, Virzi' Mariotti G, et al. A new theoretical approach on teenage cyclist-vehicle crash. *WSEAS Trans Appl Theor Mech* 2016; 11: 192–202.

53. Shen J and Jin XL. Improvement in numerical reconstruction for vehicle: pedestrian accidents. *Proc IMechE Part D: J Automobile Engineering* 2008; 222: 25–39.

54. Carollo F, Naso V, Virzi' Mariotti G, et al. Influence of the vehicle front shape in teenage cyclist-vehicle crash. *Int J Transport Syst* 2016; 1: 108–116.

55. Chakravarthy B, Lotfipour S and Vaca FE. Pedestrian injuries: emergency care considerations. *Cal J Emerg Med* 2007; 8: 15–21.

56. Schmitt KU, Niederer PF, Muser MH, et al. *Trauma biomechanics: accidental injury in traffic and sports*. London: Springer, 2007.

57. Nahum AM and Melvin JW. *Accidental injury: biomechanics and prevention*. London: Springer, 2001.

58. Schneck DJ and Bronzino JD. *Biomechanics principle and applications*. USA: CRC Press, 2008.

59. DeSantis Klinich K. *Biomechanics of pedestrian injuries related to lower extremity injury assessment tools: a review of the literature and analysis of pedestrian crash database*. University of Michigan, Transportation Research Institute, 2003.

60. Ptaka M, Rusinski E, Karlinski J, et al. Evaluation of kinematics of SUV to pedestrian impact: lower leg impactor and dummy approach. *Arch Civ Mech Eng* 2012; 12: 68–73.

61. Gazzola F. *Analisi matematica 2*, Ladotta, Bologna, 2016.

Appendix I

Notation

a	derivative of the tangent to both the curves
A_{max}	maximum acceleration
AGE	age of the test subject [years]
g	acceleration due to gravity
gt	highest acceleration
H	bumper or bonnet height
m_c	pedestrian mass
m_v	vehicle mass
Mstd	standard mass of 75 kg
RIBy	maximum of the absolute value of the lateral acceleration of the fourth or eighth rib on the hit side (units of g)
R(t)	resulting linear acceleration (units of g)
R^2	variance
T12y	maximum absolute value of the lateral acceleration of the 12th thoracic vertebra (units of g)
V	vehicle impact speed
V_{xc}	pedestrian speed in the x direction
V_{xv}	vehicle speed in the x direction
V_{yc}	pedestrian speed in the y direction
V_{yv}	vehicle speed in the y direction
V_{zc}	pedestrian speed in the z direction
V_{zv}	vehicle speed in the z direction
V_c	pedestrian speed after the impact
V_v	vehicle speed after the impact
x	vehicle motion direction
X	normalized vehicle speed $= V_v/V$
X_0	abscissa of the working point
X'	transformed abscissa
X_0'	abscissa of the working point $= 1$
y	transverse direction
Y	normalized pedestrian speed $= V_c/V$
Y_0	ordinate of the working point
Y'	transformed ordinate
Y_0'	ordinate of the working point $= 1$
z	vertical direction
α	bonnet angle
β	directional cosine x-z $= V_{xv}/V_v$
λ	Lagrange multiplier